Available online at www.sciencedirect.com
SCIENCE DIRECT
Polymer 46 (2005) 8483–8493
polymer
www.elsevier.com/locate/polymer

Modeling RAFT polymerization kinetics via Monte Carlo methods: cumyl dithiobenzoate mediated methyl acrylate polymerization

Marco Drache[a], Gudrun Schmidt-Naake[a], Michael Buback[b], Philipp Vana[b,*]

[a]*Institut für Technische Chemie, Technische Universität Clausthal, Erzstr. 18, D-38678 Clausthal-Zellerfeld, Germany*
[b]*Institut für Physikalische Chemie, Georg-August-Universität Göttingen, Tammannstr. 6, D-37077 Göttingen, Germany*

Received 4 November 2004; accepted 29 November 2004
Available online 9 June 2005

Abstract

Cumyl dithiobenzoate (CDB) mediated methyl acrylate (MA) bulk polymerizations at 80 °C, using CDB concentrations between 1.5×10^{-2} and 5.0×10^{-2} mol L^{-1}, were modeled via a novel Monte Carlo simulation procedure with respect to experimental time-dependent conversions, X, number average molecular weights, M_n, and weight average molecular weights, M_w. The simulations were based upon individual treatment of 5×10^8 discrete molecules in accordance to their actual reaction pathways. The kinetic scheme employed includes termination reactions of intermediate RAFT radicals with propagating radicals and reaction steps of the RAFT pre-equilibrium, which are different from those of the RAFT main equilibrium. The equilibrium constant of the main equilibrium of the CDB/MA system at 80 °C was found to be $K=1.2\times10^4$ L mol^{-1}, indicating a relatively stable intermediate radical. The concentration of the intermediate RAFT radical, although not employed as experimental input data for the modeling, was calculated by using the obtained set of kinetic parameters as being in excellent agreement with experimental electron spin resonance spectroscopic data.

Keywords: Reversible addition fragmentation chain transfer (RAFT) polymerization; Monte Carlo simulations; Polymerization kinetics

1. Introduction

The last few years have witnessed a rapid development of living/controlled radical polymerization processes, which permit the formation of narrowly distributed polymeric materials with controlled molecular weights and complex macromolecular architectures. The most prominent of these techniques are the nitroxide-mediated polymerization (NMP) [1,2], the atom transfer radical polymerization (ATRP) [3–5], and the reversible addition fragmentation chain transfer (RAFT) polymerization [6,7]. The RAFT process has proven to be extremely versatile with respect to monomer types and reaction conditions and developed into a highly attractive method for generating novel materials with unrivaled properties. The mediating agents employed in most RAFT polymerizations are dithioesters with the general structure Z–C(=S)S–R, which have been designed in great structural variety with respect to the leaving group (R-group) and to their stabilizing moiety (Z-group). The RAFT polymerization proceeds via a degenerative chain transfer mechanism in which two equilibria (Scheme 1) are superimposed on a conventional radical polymerization scheme with the elementary reactions, i.e. initiation, propagation and termination [8], being unaffected. Addition of a growing macroradical to the sulfur–carbon double bond of the initial dithioester compound **1** produces a carbon-centered intermediate radical **2**, which subsequently undergoes β-scission reactions to either yield back the reactants or to generate an initiating radical $R^{\cdot}$ and a polymeric dithioester compound **3**. This sequence of reactions is termed pre-equilibrium. Analogous reactions constitute the main equilibrium, in which a growing macroradical reacts with the polymeric RAFT agent **3** in a degenerative manner, i.e. reactants and products are chemically virtually identical. Recurring reversible addition fragmentation chain transfer events throughout the polymerization induce an equilibrium between dormant and living chains, which results in the living/controlled nature of the polymerization process.

Following the reaction scheme depicted in Scheme 1, the radical concentration is not influenced by the RAFT

* Corresponding author. Tel.: +49 551 3912753; fax: +49 551 393144.
E-mail address: pvana@uni-goettingen.de (P. Vana).

0032-3861/$ - see front matter © 2005 Elsevier Ltd. All rights reserved.
doi:10.1016/j.polymer.2004.11.117

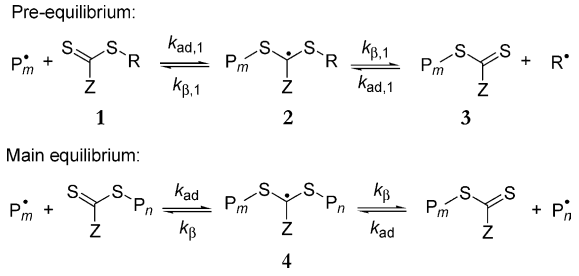

Scheme 1. Basic reaction steps of the RAFT process.

process, hence, the overall rate of polymerization remains unchanged in the ideal case of instantaneous fragmentation of the intermediate RAFT radical. However, inhibition, i.e. prolonged time periods in the initial reaction phase without significant polymerization activity, and retardation, i.e. reduction of polymerization rates in comparison to the conventional polymerization, are frequently observed. Both effects are depending in extent on the initial RAFT agent concentration. Two school of thoughts have emerged to explain these rate altering effects: (i) the fragmentation reaction of the intermediate RAFT radical is considered to be very slow [9,10], or (ii) additional side reactions, such as termination reactions of the intermediate RAFT radical with either growing macroradicals (cross-termination) or among themselves (self-termination) (Scheme 2), are held responsible for the reduction of propagating radical concentration [11–13].

A wide variety of advanced techniques has been applied to elucidate the detailed mechanism of RAFT polymerization, especially focusing on the dithiobenzoate-mediated polymerizations. High-level ab initio molecular orbital calculations [14,15] and modeling strategies based on the kinetic scheme without the assumption of any side reactions predicted fairly stable intermediate RAFT radicals with average lifetimes of seconds, and long-lived radical sinks has indeed been observed in some RAFT systems via

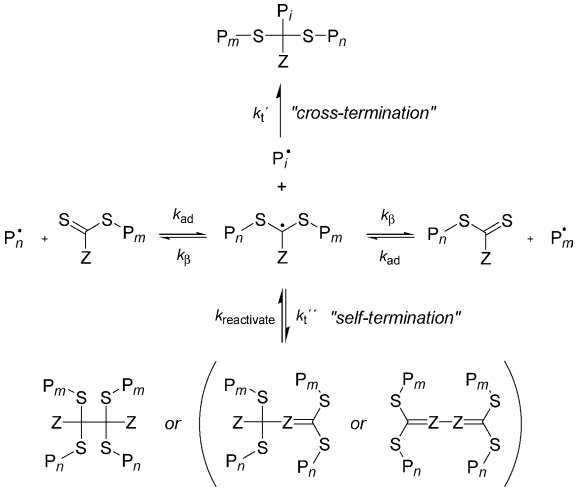

Scheme 2. Extended RAFT reaction scheme including termination of the intermediate RAFT radical.

γ-radiation-induced polymerizations [16,17]. However, the predicted remarkably high concentrations of the intermediate RAFT radical could not be confirmed via electron spin resonance (ESR) spectroscopy [12,18,19] and smaller stabilities of the intermediate RAFT radicals were consequently concluded. Termination products originating from side reactions of the intermediate RAFT radical, including recombination products via coupling of the Z-group in case of Z is phenyl (Scheme 2) [20], could be identified from model systems via nuclear magnetic resonance (NMR) spectroscopy [21,22], matrix assisted laser desorption ionization (MALDI) mass spectrometry (MS) [23], and size-exclusion chromatography [12], supporting the theory of termination of intermediate RAFT radicals being responsible for rate retardation in some RAFT systems. However, these products could not be observed from actual polymerizing systems using electrospray ionization (ESI) MS [24] or MALDI-MS [23]. In an attempt to reconcile the experimental findings, a reversible termination of the intermediate radical has been hypothesized [20,25], which, however, has yet to be confirmed.

The complexity of the RAFT process with its multitude of coupled elementary reactions has been met via modeling strategies from the very beginning of studies into RAFT kinetics. A straightforward approach to directly determine individual rate coefficients, e.g. like the pulsed-laser polymerization techniques for assessing propagation rate coefficients [26] and termination rate coefficients [27], respectively, has not yet emerged for the kinetic parameters governing the RAFT equilibrium, i.e. k_{ad} and k_{β}. These kinetic coefficients may, however, be deduced via modeling experimental data, like rate of polymerization, molecular weight data, and full molecular weight distributions, using known kinetic parameters as input values in conjunction with a specific kinetic scheme. Thus, the obtained data are model-dependent, which explains the tremendous difference of reported values of k_{ad} and k_{β} in literature [10,13].

Modeling RAFT polymerizations serves two important tasks: (i) simulation of the polymerization process using the obtained parameter set within a given kinetic scheme may substitute for complicated and time-consuming experiments, and (ii) it may additionally help to elucidate the mechanisms by providing kinetic data that may be judged against experimental results for plausibility.

Most of the simulations of RAFT polymerizations performed are based on numerical integration algorithms for solving the underlying ordinary differential equation system describing mass balances. PREDICI®, for instance, which employs a so-called discrete Galerkin h-p-method for the numerical solution of countable differential equations [28], has been used by Barner-Kowollik et al. to model cumyl dithiobenzoate (CDB) mediated styrene bulk polymerization [9] as well as cumyl phenyldithioacetate (CPDA) mediated styrene bulk and methyl methacrylate bulk polymerization [25]. These modeling studies were based upon the kinetic scheme originally proposed by the CSIRO

group [29] and with a simple transfer reaction substituting for the pre-equilibrium. Later, systematic studies into the influence of rate coefficients governing the pre- and main equilibrium and of initiator concentration, both on the resulting molecular weight distribution and polymerization rate, have been performed via PREDICI simulations by Vana et al. [30]. In that study, individual reaction steps for describing the pre-equilibrium, hence, allowing for simulations of inhibition phenomena, have been introduced. It should be noted that the RAFT equilibrium reactions are implemented into PREDICI via introduction of two virtual species, which basically represent the individual polymeric arms of the intermediate RAFT radical. This approach has recently been proven correct with respect to the concentration of the individual participating species by Wulkow and coworkers [31], however, information about how these arms are interlinked is not available.

Wang and Zhu [32,33] used the method of moments to simulate RAFT polymerizations employing a prearranged set of kinetic coefficients and performed studies into the influence of several kinetic parameters on the obtained moments of polymeric species. Pre- and main equilibrium where not treated individually. Such a momentum method approach reduces complexity significantly; however, full molecular weight distributions cannot be obtained.

Monte Carlo methods were found to be effective tools for the simulation of kinetics and full molecular weight distributions of conventional radical polymerization processes, e.g. pulsed-laser polymerizations [34–36] and olefin polymerizations including branching effects [37]. These methods are especially advantageous when detailed information about polymeric microstructure, e.g. comonomer sequence in terpolymers [38], are required. For the simulation of controlled radical polymerization, Monte Carlo methods have been employed describing NMP [39–41]. Prescott [42] used a Monte Carlo method for investigating influences of chain-length dependent termination in RAFT emulsion polymerizations using a simplified kinetic model, mainly focusing on chain-length dependent propagation and termination probabilities without studying time-dependent concentrations of individual species.

In this work, we present a novel Monte Carlo method (termed mcPolymer), which enables the comprehensive simulation of RAFT polymerizations in an extremely straightforward manner. During this simulation procedure each single molecule from a huge initial batch of molecules is accounted for throughout the entire simulated polymerization. The probability of a molecule following a distinct reaction pathway is calculated on the basis of pseudo-random numbers. This approach enables uncomplicated implementation of reactions leading to species with sophisticated macromolecular architectures and is therefore especially suited for simulation of RAFT polymerizations, where polymeric molecules with two (intermediate RAFT radical), three (cross-termination product) and four individual arms (self-termination product) possibly occur. The full molecular weight distributions of all the resulting polymeric materials are directly accessible. The RAFT equilibrium reactions (Scheme 1) and additional side reactions (Scheme 2) are calculated directly according to their chemical reaction pathways and without the necessity of virtual species.

We employed this powerful simulation tool for modeling the CDB-mediated methyl acrylate (MA) bulk polymerization at 80 °C, which is known to exhibit a pronounced rate retardation effect [43]. This strong retardation renders the CDB/MA system an interesting candidate for studies into RAFT kinetics. The objectives of the present work are to introduce the new Monte Carlo simulation procedure and to apply it for the estimate of model-dependent rate coefficients via modeling experimental kinetic data, i.e. time-resolved average molecular weight and monomer conversion data. The significance of the modeling result was explored by comparing simulated and experimental results with respect to both molecular weight distributions and concentrations of the intermediate RAFT radical, which were obtained via electron spin resonance (ESR) spectroscopy.

2. Computational methods

The simulations were initialized with a predetermined total number of 5×10^8 to 5×10^{10} individual molecules, which were assigned to the reactant species, i.e. monomer, RAFT agent, and initiator, according to their molar concentrations in the initial reaction mixture. A single Monte Carlo step performed reflects the individual reaction of a discrete molecule according to the kinetic scheme assumed. Prior to each Monte Carlo step the reaction probability, p_i, for each possible reaction, i, is calculated from the product of the stochastic reaction rate coefficient and the active number of reactant molecules, which are involved in that reaction. The time steps of the simulation were implemented as being variable. Combination of the sum over all reaction probabilities, p_i, with a uniformly distributed random number, r, gives the time interval τ (Eq. (1)),

$$\tau = \frac{1}{\sum_i p_i} \ln \frac{1}{r} \tag{1}$$

which describes the time required for one Monte Carlo step.

From all possible reaction pathways, reaction i is selected by using another random number and the individual reaction probability, p_i. This reaction was subsequently executed by increasing the number of product molecules and simultaneously decreasing the number of reactant molecules, with distinct chain lengths being transferred from reactants to products in the case of polymeric species being involved.

In order to facilitate computational operation, templates describing reactions between reactants with comparable

characteristics were designed. Reactions of similar nature, e.g. termination via combination, addition of propagating radicals toward polymeric RAFT agent, and cross-termination, may hence be calculated using the same universal reaction template for combining two polymeric species, by which all chain lengths of the reactants are individually preserved in the product molecule.

The variation of kinetic coefficients that may change during the progression of the polymerization process, e.g. by temperature variation or by increasing monomer conversion, is considered. The adjustment is not made after each time interval, τ, but after a predetermined reaction time period of typically 60 s, in order to reduce computational time.

The Monte Carlo simulation procedure was executed by the mcPolymer program (Windows and Linux), programmed in C++ with a Tcl-interface, and employing the Mersenne Twister high-level 623-dimensionally equidistributed uniform pseudo-random number generator [44]. The calculations were performed on a computer cluster comprising 20 CPUs (AMD Athlon XP 1900+ to AMD Athlon 64 3200+), running under SuSE-Linux. Simulations were independent and could therefore be executed in parallel. The job-generator used for the automated execution of the simulations was implemented as a Tcl-script, starting the jobs via the Grid Engine© cluster queue system by Sun Microsystems.

The computational time was depending on the rates of the participating reactions, that is, increasing reaction probability directly reduces the time interval per Monte Carlo step (Eq. (1)). As a consequence, a larger number of calculations had to be carried out for describing the same reaction time period in case of fast reaction rates. Overall calculation times were found to be especially sensitive to the absolute reaction rates of the addition and fragmentation reactions of the RAFT equilibrium. Additionally, the computational time was increasing at higher RAFT agent concentrations, because the absolute number of polymer chains participating in the time consuming RAFT equilibrium is increased.

3. Experimental section

3.1. Materials

Methyl acrylate (Fluka, $\geq$99%) was purified by passing through a column filled with basic Al_2O_3 and subsequent distillation under reduced pressure. The initiator 2,2′-azobis(*iso*-butyronitrile) (AIBN, Merck) was used as received; the purity was more than 99% as verified by ^{1}H NMR analysis. The RAFT agent cumyl dithiobenzoate was synthesized according to the procedure detailed earlier [43]. The purity of the RAFT agent was more than 98% as verified by ^{1}H NMR analysis. 2,2,6,6-Tetramethyl-piperidine-*N*-oxyl radical (TEMPO, 99%, Aldrich) for ESR calibration was used without further purification. Tetrahydrofuran for size-exclusion chromatography (THF, Carl Roth, Rotipuran, stabilized with 2,6-di-*tert*-butyl-4-methylphenol) was used as received.

3.2. Polymerizations

Stock solutions of MA (25 mL), AIBN ([AIBN] = 1.0×10^{-2} mol L^{-1}) and cumyl dithiobenzoate with initial concentrations of 1.5×10^{-2}, 2.5×10^{-2}, and 5.0×10^{-2} mol L^{-1} were prepared. Five samples of each stock solution were transferred to glass vials, sealed with teflon/rubber septa, and thoroughly deoxygenated by purging with nitrogen gas for approximately 10 min. The vials were subsequently inserted into a block heater thermostated at 80 $\pm$ 0.1 °C. Samples were removed after 15, 30, 45, 60 and 75 min, respectively. The reactions were stopped by cooling the solutions in liquid nitrogen. The polymeric product was isolated by evaporating off the residual methyl acrylate. Monomer conversions, X, were determined gravimetrically.

3.3. ESR measurements

Electron spin resonance spectra were recorded on a Bruker Elexsys® E-500 CW-ESR spectrometer. Absolute radical concentrations were obtained via calibration with TEMPO solutions in methyl acrylate of known concentrations and under conditions as close as possible to those of the actual polymerization experiment. In order to improve the signal-to-noise ratio, up to 200 individual spectra were co-added.

3.4. Molecular weight analysis

Molecular weight distributions were determined by means of size-exclusion chromatography (SEC) using a Waters 712 WISP autosampler, a Waters 515 HPLC pump, PSS-SDV columns with nominal pore sizes of 10^5, 10^3 and 10^2 Å, a Waters 2410 refractive index detector, and THF at 35 °C as the eluent. The SEC set-up was calibrated against polystyrene (PS) standards of narrow polydispersity (M_p = 410–2,000,000 g mol^{-1}) from Polymer Standards Service. Mark–Houwink parameters for poly(MA) in THF (K = 1.95×10^{-2} mL g^{-1}, a = 0.660) [45] provided access to absolute molecular weight distributions according to the principle of universal calibration [46].

4. Kinetic model

The kinetic model underlying the modeling of the RAFT polymerization is presented in Scheme 3.

The upper part of the reaction scheme comprises the basic conventional reaction steps of a radical polymerization, i.e. initiation, propagation and termination.

MA Polymerization

Initiation

$$\text{AIBN} \xrightarrow{k_d} 2f \times I^{\bullet}$$

$$I^{\bullet} + \text{MA} \xrightarrow{k_p} P_1^{\bullet}$$

Propagation

$$P_n^{\bullet} + \text{MA} \xrightarrow{k_p} P_{n+1}^{\bullet}$$

Termination

$$P_n^{\bullet} + P_m^{\bullet} \xrightarrow{k_{t,c}} D_{n+m}$$

RAFT-specific reaction steps

Pre-equilibrium

$$P_m^{\bullet} + \text{RAFT} \underset{k_{\beta,1}}{\overset{k_{ad,1}}{\rightleftharpoons}} \text{Int}_{m,1}^{\bullet}$$

$$\text{Int}_{m,1}^{\bullet} \underset{k_{ad,1}}{\overset{k_{\beta,1}}{\rightleftharpoons}} \text{polyRAFT}_m + R^{\bullet}$$

Re-initiation

$$R^{\bullet} + \text{MA} \xrightarrow{k_p} P_1^{\bullet}$$

Main equilibrium

$$P_m^{\bullet} + \text{polyRAFT}_n \underset{k_{\beta}}{\overset{k_{ad}}{\rightleftharpoons}} \text{Int}_{m,n}^{\bullet}$$

$$\text{Int}_{m,n}^{\bullet} \underset{k_{ad}}{\overset{k_{\beta}}{\rightleftharpoons}} \text{polyRAFT}_m + P_n^{\bullet}$$

Cross-termination

$$\text{Int}_{m,1}^{\bullet} + P_n^{\bullet} \xrightarrow{\alpha \times k_{t,c}} \text{D-int}_{1,m+n}$$

$$\text{Int}_{m,n}^{\bullet} + P_k^{\bullet} \xrightarrow{\alpha \times k_{t,c}} \text{D-int}_{m+n+k}$$

Scheme 3.

Termination is assumed to proceed exclusively via combination, the dominant termination mode in methyl acrylate polymerization [47]. The associated kinetic coefficients are taken from literature and can be found in Table 1.

The RAFT reaction sequences, which are inducing the equilibrium between active and dormant radicals, are implemented directly according to their reaction pathways as shown in Scheme 1. In order to minimize the multitude of fit parameters, the reinitiation of the expelled leaving group radical, $R^{\bullet}$, is assumed to proceed with the same rate as the propagation step. Addition rate coefficients being larger than k_p would not significantly affect kinetics, lower addition rates, however, may induce inhibition effects [30,48]. Because it is beyond the scope of the present work to investigate inhibition effects in detail (Section 5), we chose this basic approach. It should, however, be stressed that distinction between the pre- and main equilibrium is vital for inducing an induction period. The individual addition and fragmentation reactions of the pre-equilibrium, $k_{ad,1}$ and $k_{\beta,1}$, were thus assumed as being independent of those of the main equilibrium, k_{ad} and k_{β}. The kinetic model additionally contains termination of the intermediate RAFT radical with the propagating radical (cross-termination) via combination as working hypothesis. The rate coefficient of such reaction is described by $\alpha \times k_{t,c}$. It should be noted that self-termination of the intermediate RAFT radical is not included into the kinetic model used in this initial study in order to minimize complexity, however, modeling based on kinetic schemes with increased complexity are currently underway.

5. Results and discussion

Three independent CDB-mediated MA bulk polymerization experiments at 80 °C, with initial RAFT agent concentrations of 1.5×10^{-2}, 2.5×10^{-2} and 5.0×10^{-2} mol L^{-1}, respectively, and an initial AIBN concentration of 1.0×10^{-2} mol L^{-1} were performed and analyzed with respect to time-dependent monomer conversions, X, number average molecular weights, M_n, and weight average molecular weights, M_w, which are listed in Table 2 and depicted in Figs. 1 and 2.

Four important features of these polymerizations can be identified:

(i) The polymerization reaction is comparatively fast, due to the relatively high initiator concentration, the high decomposition rate of AIBN at 80 °C, and the high propagation rate of MA (Table 1). Fifty percent of monomer conversion is achieved after only 1 h when employing 1.5×10^{-2} mol L^{-1} CDB.

(ii) The polymerizations are, nevertheless, very well controlled, especially at high RAFT agent concentrations, as is obvious from the low polydispersity indices, PDI, ($1.09 < \text{PDI} = M_w/M_n < 1.36$, depending

Table 1
Kinetic input parameters for the Monte Carlo modeling of CDB-mediated MA bulk polymerization at 80 °C

Monomer	$[MA]_0 = 10.3$ mol L^{-1}	
RAFT agent	$[CDB]_0 = 1.5\times10^{-2}$; 2.5×10^{-2}; 5.0×10^{-2} mol L^{-1}	
Initiation	$[AIBN]_0 = 1\times10^{-2}$ mol L^{-1}	
	$k_d = 1.58\times10^{-4}$ s^{-1}	[53]
	$f = 0.64$	[54]
Propagation	$k_p = 31{,}800$ L mol^{-1} s^{-1}	[45]
Termination	$k_{t,c} = \exp(19.5–3.7\times X)$ L mol^{-1} s^{-1}	[55]

Table 2
Experimental data (reaction time, t, monomer conversion, X, number average molecular weight, M_n, weight average molecular weight, M_w, and polydispersity index, PDI) and theoretical number average molecular weight, M_n^{theo}, for CDB-mediated MA bulk polymerization at 80 °C using 1×10^{-2} mol L^{-1} AIBN as the initiator

[CDB] (mol L^{-1})	t (min)	X (%)	M_n (g mol^{-1})	M_n^{theo} (g mol^{-1})	M_w (g mol^{-1})	PDI
1.5×10^{-2}	15	11.1	7793	7089	8546	1.10
	30	28.6	19,198	18,209	24,045	1.25
	45	41.9	27,648	26,701	35,423	1.28
	60	53.0	35,855	33,755	46,773	1.30
	75	60.8	39,954	38,696	54,333	1.36
2.5×10^{-2}	15	5.5	1796	2105	1994	1.11
	30	17.4	6541	6633	7379	1.13
	45	27.7	10,756	10,582	12,601	1.17
	60	35.9	13,766	13,703	16,595	1.21
	75	44.6	17,290	17,028	21,919	1.27
5.0×10^{-2}	15	2.0	222	389	243	1.10
	30	7.0	1118	1345	1234	1.10
	45	13.4	2297	2553	2534	1.10
	60	19.3	3539	3692	3875	1.09
	75	25.3	4756	4835	5303	1.12

on monomer conversion and CDB concentration) and from the steadily increasing M_n values with progressive monomer conversion.

(iii) The polymerization rate is significantly lowered with increasing CDB concentration, i.e. rate retardation is operative. The monomer conversion after 1 h, for instance, is reduced from 53% when using 1.5×10^{-3} mol L^{-1} CDB to only 19% with 5.0×10^{-3} mol L^{-1} CDB.

(iv) A pronounced inhibition period, in extent being dependent on the initial RAFT agent concentration, occurs, that is, no polymerization activity is observed in the initial time period.

The experimental data sets were subsequently modeled according to the kinetic scheme described in Section 4 using the mcPolymer program, with the fit parameters $k_{ad,1}$, $k_{\beta,1}$, k_{ad}, k_β, and α (Scheme 3). The determination of the optimum kinetic parameter set, describing the experimental results appropriately, was demanding, because of the coupled individual RAFT reaction steps. Manual optimization of the kinetic parameters via personal validation of the simulation results against the experimental data and repeated adjustment of the input fit parameters did not succeed. On the other hand, the systematic variation of all five fit parameters in a significantly large search space using a relatively narrow grid would have required an unacceptably large number of individual simulations.

We therefore performed a stochastic scan of a parameter space with initial limits selected on the basis of rational considerations and preliminary simulation results. Simulations of polymerizations via the mcPolymer program, using a random combination of kinetic parameters, were performed via an automated job generator for all three experimental initial RAFT agent concentrations up to reaction times of 100 min and using an initial number of 5×10^8 molecules. The deviations of simulated time-dependent conversions and average molecular weights

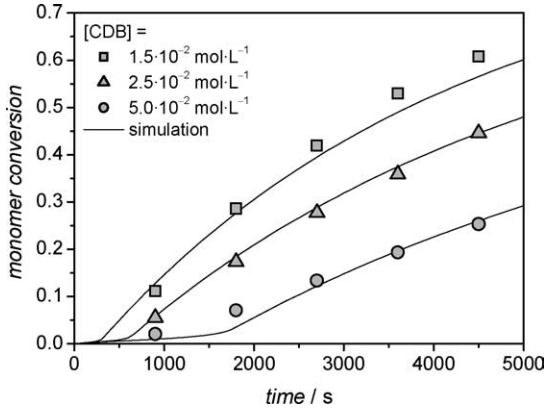

Fig. 1. Experimental and simulated monomer conversion vs. reaction time for CDB-mediated MA bulk polymerization at 80 °C, using different initial CDB concentrations and AIBN ([AIBN] = 1.0×10^{-2} mol L^{-1}) as the initiator.

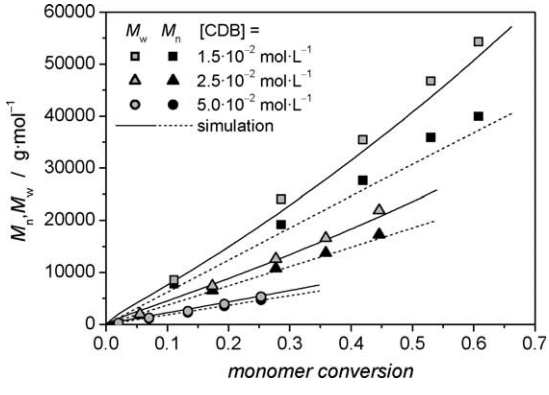

Fig. 2. Experimental and simulated number average molecular weight, M_n (full symbols), and weight average molecular weight, M_w (open symbols), vs. monomer conversion for CDB-mediated MA bulk polymerization at 80 °C, using different initial CDB concentrations and AIBN ([AIBN] = 1.0×10^{-2} mol L^{-1}) as the initiator.

from the experimental data were subsequently automatically assessed via error sums. Three individual optimization runs with successive reduction of the parameter window size around the optimum results (Table 3) were performed, resulting in an overall number of 7500 simulations. The calculation of one single MA RAFT polymerization experiment with 100 min reaction time and using, e.g. 5×10^{-2} mol L^{-1} CDB, corresponded to 8.95×10^{8} Monte Carlo steps and 14 min computational time on an AMD Athlon 64 3200+ CPU, with a maximum memory requirement of 118 MB. Overall calculation time on a cluster of 20 computers was approximately 20 days, which is equivalent to more than 1 year of absolute computational time.

The resulting optimum set of kinetic parameters, obtained from simultaneous fitting of rate and molecular weight data, is presented in Table 4.

The simulated conversion vs. time plots for three CDB concentrations using the input and modeled kinetic parameters of Tables 1 and 4 are depicted in Fig. 1 together with the experimentally obtained data. The simulations almost perfectly match the experimental findings. Simulated evolution of average molecular weights, M_n and M_w, respectively, with monomer conversion is shown in Fig. 2, also demonstrating the excellent agreement between simulated and experimental results.

The comparison of simulated and calculated full molecular weight distributions (Fig. 3), e.g. of polymeric material originated from MA RAFT polymerization with 5.0×10^{-2} mol L^{-1} CDB after 25% monomer conversion, indicates a very good match. Minor deviations can be seen in the high molecular weight regime. This might either be due to the Gaussian broadening of the SEC instrument or due to imperfect SEC calibration at high molecular weights, where termination products of the intermediate RAFT radical with branched microstructure (e.g. three-arm star) may occur.

The obtained k_{ad} and k_β values describing the main equilibrium result in an equilibrium constant of $K=k_{ad}/k_\beta=$ 11,900 L mol^{-1} (Table 4). This value is three orders of magnitude higher than the one reported for CDB-mediated styrene polymerization at 60 °C ($K_{CDB/styrene}=55$ L mol^{-1} [12]), which has also been derived on the basis of a kinetic scheme that includes irreversible cross-termination of the intermediate radical. The comparatively high value of K in the CDB/MA system is indicative of a relatively stable intermediate RAFT radical and demonstrates the very strong influence of the monomer derived leaving group on the average lifetime of such radicals. This has recently been demonstrated by Coote [15] via high-level ab initio calculations of small model radicals, which indicated that the equilibrium constant K is extremely sensitive to the R-groups considered, covering a range of four orders of magnitude with Z being phenyl.

Table 4
Optimum set of parameters for the kinetic model detailed in Section 4, describing the RAFT equilibrium reactions of a CDB-mediated MA bulk polymerization at 80 °C

Pre-equilibrium
$k_{ad,1}=3.06\times10^{8}$ L mol^{-1} s^{-1}
$k_{\beta,1}=20.9$ s^{-1}
$K_1=1.46\times10^{7}$ L mol^{-1}
Main equilibrium
$k_{ad}=9.36\times10^{6}$ L mol^{-1} s^{-1}
$k_\beta=784$ s^{-1}
$K=1.19\times10^{4}$ L mol^{-1}
$\alpha=0.15$

It has been demonstrated earlier that at a given value of K the polydispersity of the resulting polymer is determined by the individual values of k_{ad} and k_β. The higher the absolute values of k_{ad} and k_β, the smaller the resulting PDI [30]. The polydispersity is therefore a direct measure for the successful modeling of these kinetic coefficients. The PDI, however, exhibits an enhanced relative error, because it is composed of two measured values, and its accurate determination is additionally limited by the Gaussian broadening of the SEC. Thus, the absolute values of the modeled k_{ad} and k_β values are considered exhibiting a higher uncertainty than the resulting equilibrium constant, K, which is also determined by the experimental rate data. It should be noted that individual treatment of M_n and M_w, instead of employing PDI as experimental quantity, increased the accuracy of the resulting fit parameters.

The optimum α value of 0.15 obtained via the modeling

Table 3
Parameter intervals for the stochastic modeling procedure

	Run 1	Run 2	Run 3
Number of jobs	1000	1000	500
$k_{ad,1}$ (min)/L mol^{-1} s^{-1}	1.0×10^{7}	8.0×10^{7}	3.0×10^{8}
$k_{ad,1}$ (max)/L mol^{-1} s^{-1}	5.0×10^{8}	5.0×10^{8}	5.0×10^{8}
$k_{\beta,1}$ (min)/s^{-1}	1.0×10^{0}	1.0×10^{1}	2.0×10^{1}
$k_{\beta,1}$ (max)/s^{-1}	1.0×10^{2}	5.0×10^{1}	4.0×10^{1}
k_{ad} (min)/L mol^{-1} s^{-1}	6.0×10^{6}	6.0×10^{6}	9.0×10^{6}
k_{ad} (max)/L mol^{-1} s^{-1}	3.0×10^{7}	1.2×10^{7}	1.3×10^{7}
k_β (min)/s^{-1}	1.0×10^{2}	1.0×10^{2}	7.0×10^{2}
k_β (max)/s^{-1}	2.0×10^{4}	1.0×10^{3}	8.0×10^{2}
α (min)	0.05	0.12	0.13
α (max)	0.20	0.17	0.17

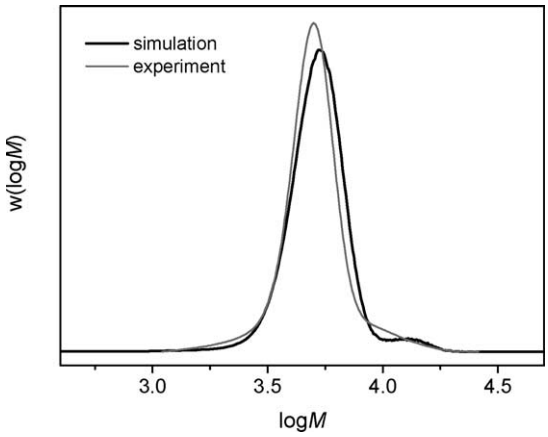

Fig. 3. Experimental and simulated normalized chain-length distributions (SEC-curves) of CDB-mediated MA bulk polymerizations ([CDB] = 5×10^{-2} mol L^{-1}) at 80 °C, after 25% monomer conversion using AIBN as the initiator ([AIBN] = 1.0×10^{-2} mol L^{-1}).

is below the value of 0.5 determined for the CDB-mediated styrene bulk polymerization at 60 °C [49]. This might be understood by an increased relative steric influence in the case of MA, where the conventional termination reaction between two growing radicals is considered being essentially unaffected by steric hindrance. The relative lowering of the termination rate coefficient, when comparing conventional to cross-termination, may therefore be greater in MA than in the styrene system, with its sterically more demanding styryl-radicals.

It should be noted that implementation of a pre-equilibrium with kinetic coefficients being independent of those of the main equilibrium was necessary to successfully model the experimentally observed induction period. Such inhibition has often been observed in dithiobenzoate mediated acrylate polymerizations and has either been attributed to stable first intermediates [43] or slow propagation of the initiating and leaving group radical [48]. For our studies we chose a kinetic picture of increased stability of the first intermediate radical in conjunction with irreversible cross-termination in order to induce the induction period. Such an approach exhibits the closest kinetic similarity to the mechanism assumed for the main equilibrium. Alternatively, the induction period may, for instance, be described via an increased α value for the pre-equilibrium, representing an increased termination probability of small radicals. However, it should be noted that the evidence found for the main equilibrium (see below) is not affected by using different models describing the pre-equilibrium.

Although it is beyond the scope of the present work to investigate the initial period in detail, it is interesting to note that the obtained value of K_1 for the pre-equilibrium of 1.46×10^{7} L mol^{-1} is only one order of magnitude different from the value of 1.5×10^{6} predicted by ab initio calculations for a very similar radical, namely, the dithioester intermediate radical with a methyl and $-CH_2COOCH_3$ leaving group substituent [15]. Modeling of the pre-equilibrium employing kinetic schemes with increased complexity in conjunction with experimentally determined time-resolved concentrations of participating species, such as the initial RAFT agent, is currently underway.

It should be noted that the obtained parameters (Table 4) are model-dependent, that is, they are only valid for the kinetic model described in Section 4. Equally good modeling results of monomer vs. time and average molecular weight vs. time data may be obtained assuming a different kinetic model, e.g. one which assumes absence of irreversible termination reactions of intermediate RAFT radicals, with resulting kinetic parameters being largely different from the ones for the model presented here. Model discrimination between competing theories is consequently not feasible by only considering time-dependent conversion and molecular weight data.

In order to probe the significance of the kinetic model and the related kinetic coefficients we acquired additional experimental data by determining time-dependent concentrations of radicals present in the polymerizing system via ESR. The ESR spectrum obtained from a CDB-mediated MA bulk polymerization at 80 °C is shown in Fig. 4 and can be attributed to the corresponding intermediate RAFT radical.

A very similar spectrum has recently been observed by Chernikova et al. [50] in a dithiobenzoate mediated *n*-butyl acrylate polymerization. The radical concentration vs. time profile obtained via calibrated doubly integrated spectral areas is depicted in Fig. 5.

The measured radical concentration of approximately 1.5×10^{-6} mol L^{-1} was assumed to be entirely due to the concentration of the intermediate RAFT radical, [Int$^{\bullet}$], as the propagating radical concentration was calculated being two orders of magnitude lower, i.e. $[P_n^{\bullet}] \approx 10^{-8}$ mol L^{-1}. The concentration of the intermediate RAFT radical in the studied CDB/MA system is higher than the one observed in the CDB-mediated styrene polymerization [12,18], indicating an increased stability of the intermediate RAFT radical in case of poly(MA) being the leaving group, and both the absolute value and the evolution with time is very close to

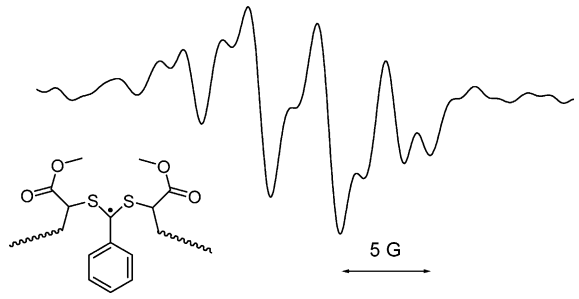

Fig. 4. ESR spectrum observed in the CDB-mediated bulk polymerization of MA at 80 °C, with AIBN being the initiator, and structure of the corresponding intermediate RAFT radical.

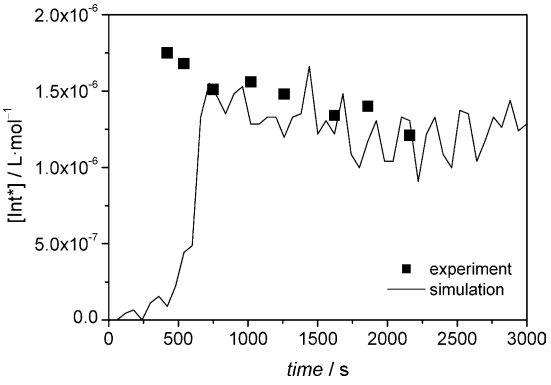

Fig. 5. Experimental (ESR) and simulated intermediate RAFT radical concentration vs. reaction time for a CDB-mediated ([CDB] = 2.5×10^{-2} mol L^{-1}) MA bulk polymerization at 80 °C, using AIBN ([AIBN] = 1.0×10^{-2} mol L^{-1}) as the initiator.

recent data obtained by Chernikova et al. for *tert*-butyl dithiobenzoate mediated *n*-butyl acrylate polymerization at 90 °C [50].

Comparison of the experimental [Int$^{\bullet}$], measured in RAFT bulk polymerization of MA at 80 °C using 2.5×10^{-3} mol L^{-1} CDB, with the simulated time-resolved data yields a striking congruence as is obvious from Fig. 5. It should be stressed that the concentration of the intermediate radical was not a fit parameter, that is, the match between experimental and simulated [Int$^{\bullet}$] is an independent indication for the significance of the chosen kinetic scheme and the obtained kinetic coefficients. It should further be noted that modeling the experimental time-resolved conversion and average molecular weight data assuming absence of termination reactions of the intermediate RAFT radicals arrives at a main equilibrium constant of $K = k_{ad}/k_{\beta} = 2.4\times10^{7}$. Such a model describes these experimental data with equal quality, however, the predicted [Int$^{\bullet}$] vs. time trace shows a steady increase with time and reaches a value of 1.6×10^{-3} mol L^{-1} after 30 min in case of [CDB] = 2.5×10^{-2} mol L^{-1}. This result is in clear contradiction to the experimental findings. We are well aware that the presented study is no independent proof of a kinetic model. However, it lends credit to the assumption that the intermediate radical may undergo side reactions that lowers the propagating radical concentration.

Very recently, Feldermann et al. [51] claimed to disprove that cross-termination of the intermediate radicals is responsible for the rate retardation in RAFT on example of the CDB-mediated styrene bulk polymerization. The authors therein demonstrated that detailed experimental conversion vs. time data cannot be adequately fitted to a model that contains cross-termination in the main equilibrium only and therefrom concluded that cross-termination does not occur at all. However, by using the kinetic model introduced above (Scheme 3), which includes a pre-equilibrium being different to the main equilibrium and which allows for cross-termination of all the intermediate radicals, the conversion vs. time traces presented by Feldermann et al. [51] can also be described perfectly, both for the low monomer conversion regime, which may be attributed to the pre-equilibrium, and for higher monomer conversions. This result demonstrates that by assuming RAFT equilibrium reactions being different for small or oligomeric radicals and by including cross-termination of the first intermediate radicals—which reaction Feldermann et al. [51] omitted—, conversion vs. time data can be described equally well by the general concept of termination of the intermediate RAFT radicals. These findings effectively invalidate the claim stated by Feldermann et al. [51] that model discrimination is possible by using conversion vs. time data alone. Additional experimental data, such as the ESR data presented above, are in fact necessary to gain further insight into the RAFT process.

The termination reaction of the intermediate RAFT radical assumed in this study continuously produces dead polymeric material, both in the pre- and in the main equilibrium. So-called three-arm stars are generated in case of termination by combination in the main equilibrium, whereas linear polymer, i.e. three-arm star polymer with the non-polymeric R-group being one arm, is formed during the pre-equilibrium. The complete number distribution vs. a linear chain-length axis for such polymeric species, D-int (Scheme 3), is depicted in Fig. 6 together with the number distribution trace of living polyRAFT agent for the MA polymerization with 5×10^{-2} mol L^{-1} CDB after 75 min and 25% monomer conversion, respectively. Here, the molar amount of cross-termination product relative to the one of the living polymeric dithioester compound is 3.4%. It should be noted that, following the optimum set of parameters, the cross-termination reaction is dominating over the conventional termination. The ratio between cross- and conventional termination, which is naturally interlinked with the α-value, may find further refinement when unambiguous assignment of the high-molecular weight

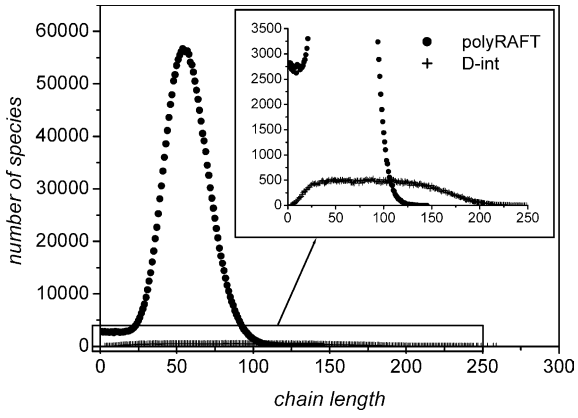

Fig. 6. Simulated absolute number of living polymeric RAFT agent (polyRAFT) and cross-termination product (D-int) vs. chain length for a CDB-mediated MA bulk polymerization ([CDB] = 5.0×10^{-2} mol L^{-1}) at 80 °C after 25% monomer conversion, using AIBN ([AIBN] = 1.0×10^{-2} mol L^{-1}) as the initiator. Total number of species: 2,185,246.

shoulder in the full molecular weight distribution to either star or linear polymer becomes possible.

Three-arm stars have indeed been experimentally found from CDB/styrene and CDB/BA model systems [12,21–23], indicating that terminating side reactions of the intermediate RAFT radical are viable reaction channels. However, these termination products could not be identified from CDB-mediated MA polymerization at low monomer conversion using SEC in conjunction with ESI-MS, hence, challenging the theory that termination of intermediate RAFT radicals is responsible for the observed rate retardation [24]. It can, however, be seen from Fig. 6 that the termination product is evenly distributed over a wide range of different chain lengths, whereas the living polymeric RAFT agent is narrowly distributed in a limited chain-length regime. This effectively reduces the molar ratio of termination products to polyRAFT species at a distinct chain length, as determined in a MS study, to less than 0.85%, e.g. at the living peak maximum in case of 25% monomer conversion. This ratio becomes smaller for lower monomer conversions, due to the cumulative production of the termination products. In addition, Venkathesh et al. [23] have recently demonstrated that separation via SEC prior to the MS detection may lead to a pronounced separation of linear and star polymer in the MS spectrum, hampering the tracing of branched termination products. However, tracking down and characterizing termination products as direct evidence for reaction pathways remain issues in RAFT and will stay in the center of scientific interest. Uncovering such termination products in polymerizing systems may be especially promising at high monomer conversions and high molecular weights, due to the cumulative nature of its production.

It should be noted that the kinetic scheme used in this study is not claimed to be complete and waits to be further refined. Additional reaction pathways may well be operational in the CDB/MA system: (i) self-termination between two intermediate radicals may become an important reaction, due to the relatively high concentration of the intermediate RAFT radical. Termination products from such a self-termination reaction have recently been identified via MALDI—besides cross-termination products—in a CDB/butyl acrylate model system [23], and recent studies into CDB-mediated MA polymerizations at 300 bar in supercritical CO_2 have also pointed toward increased self-termination [52]. (ii) Additionally, termination reactions involving the intermediate RAFT radicals may be reversible to some extent, as has been signified by radical storage effects in CDB/styrene- and CDB/MA-systems [16,17]. Such reactions, possibly proceeding over radical centers that are delocalized in an aromatic Z-group [20], may administer an additional persistent radical effect that may increase the quality of control in strongly retarded RAFT polymerization systems.

Additional experimental data, such as higher statistical moments of the chain-length distribution and complete chain-length distributions, respectively, as well as data from radical storage experiments will be employed in future modeling studies, based on more complex kinetic schemes, in order to determine to what extent such additional reaction channels may occur. It is the strength of the introduced mcPolymer program that such additional reaction pathways can be implemented with relative ease, opening up a multitude of various modeling applications and allowing for a comprehensive testing of different kinetic schemes.

6. Conclusion

A novel Monte Carlo simulation procedure, which allows for the simulation of polymerization processes with complex macromolecular architectures being present, has been developed. Time-dependent concentrations and full molecular weight distributions of all participating species are directly accessible via this simulation tool, which has been employed for modeling cumyl dithiobenzoate mediated methyl acrylate RAFT polymerization at 80 °C. The kinetic coefficients deduced for the RAFT equilibrium indicate a relatively stable intermediate radical, although a kinetic scheme including termination of the intermediate RAFT radical with propagating radicals was applied. The parameter set obtained via the modeling procedure allowed for the calculation of the concentrations of the intermediate RAFT radical, which are in excellent agreement with experimental electron spin resonance spectroscopic data.

Acknowledgements

The authors gratefully acknowledge support by the Deutsche Forschungsgemeinschaft within the framework of the European Graduate School ‘Microstructural Control In Free-Radical Polymerization’. We would like to thank Dr Toshihiko Arita for support with the polymerization experiments and Thomas Junkers for help with the ESR-measurements.

References

[1] Solomon DH, Rizzardo E, Cacioli P. EP0135280; 1985.
[2] Hawker CJ, Bosman AW, Harth E. Chem Rev 2001;101:3661–88.
[3] Kato M, Kamigaito M, Sawamoto M, Higashimura T. Macromolecules 1995;28:1721–3.
[4] Matyjaszewski K, Xia J. Chem Rev 2001;101:2921–90.
[5] Wang J-S, Matyjaszewski K. J Am Chem Soc 1995;117:5614–5.
[6] Chiefari J, Chong YK, Ercole F, Krstina J, Jeffery J, Le TPT, et al. Macromolecules 1998;31:5559–62.
[7] Barner-Kowollik C, Davis TP, Heuts JPA, Stenzel MH, Vana P, Whittaker M. J Polym Sci, Part A: Polym Chem 2003;41:365–75.
[8] Vana P, Barner-Kowollik C, Davis TP, Matyjaszewski K. In: Mark HF et al, editor. Encyclopedia of polymer science and technology, 3rd edn, vol. 11. Hoboken: Wiley-Interscience; 2003. p. 359–472.

[9] Barner-Kowollik C, Quinn JF, Morsley DR, Davis TP. J Polym Sci, Part A: Polym Chem 2001;39:1353–65.
[10] Barner-Kowollik C, Coote ML, Davis TP, Radom L, Vana P. J Polym Sci, Part A: Polym Chem 2003;41:2828–32.
[11] Monteiro MJ, de Brouwer H. Macromolecules 2001;34:349–52.
[12] Kwak Y, Goto A, Tsujii Y, Murata Y, Komatsu K, Fukuda T. Macromolecules 2002;35:3026–9.
[13] Wang AR, Zhu S, Kwak Y, Goto A, Fukuda T, Monteiro MS. J Polym Sci, Part A: Polym Chem 2003;41:2833–9.
[14] Coote ML, Radom L. J Am Chem Soc 2003;125:1490–1.
[15] Coote ML. Macromolecules 2004;37:5023–31.
[16] Barner-Kowollik C, Vana P, Quinn JF, Davis TP. J Polym Sci, Part A: Polym Chem 2002;40:1058–63.
[17] Barner L, Quinn JF, Barner-Kowollik C, Vana P, Davis TP. Eur Polym J 2003;39:449–59.
[18] Calitz FM, Tonge MP, Sanderson RD. Macromolecules 2003;36:5–8.
[19] Alberti A, Benaglia M, Laus M, Macciantelli D, Sparnacci K. Macromolecules 2003;36:736–40.
[20] Monteiro MJ, Bussels R, Beuermann S, Buback M. Aust J Chem 2002;55:433–7.
[21] Calitz FM, McLeary JB, McKenzie JM, Tonge MP, Klumperman B, Sanderson RD. Macromolecules 2003;36:9687–90.
[22] Kwak Y, Goto A, Komatsu K, Sugiura Y, Fukuda T. Macromolecules 2004;37:4434–40.
[23] Venkatesh R, Staal BBP, Klumperman B, Monteiro MJ. Macromolecules 2004;37:7906–17.
[24] Ah Toy A, Vana P, Davis TP, Barner-Kowollik C. Macromolecules 2004;37:744–51.
[25] Barner-Kowollik C, Quinn JF, Nguyen TLU, Heuts JPA, Davis TP. Macromolecules 2001;34:7849–57.
[26] Olaj OF, Bitai I, Hinkelmann F. Makromol Chem 1987;188:1689–702.
[27] Buback M, Egorov M, Junkers T, Panchenko E. Macromol Rapid Commun 2004;25:1004–9.
[28] Wulkow M. Macromol Theory Simul 1996;5:393–416.
[29] Moad G, Chiefari J, Chong YK, Krstina J, Mayadunne RTA, Postma A, et al. Polym Int 2000;49:993–1001.
[30] Vana P, Davis TP, Barner-Kowollik C. Macromol Theory Simul 2002;11:823–35.
[31] Wulkow M, Busch M, Davis TP, Barner-Kowollik C. J Polym Sci, Part A: Polym Chem 2004;42:1441–8.
[32] Wang AR, Zhu S. J Polym Sci, Part A: Polym Chem 2003;41:1553–66.
[33] Wang AR, Zhu S. Macromol Theory Simul 2003;12:196–208.
[34] Lu J, Zhang H, Yang Y. Makromol Chem, Theory Simul 1993;2:747–60.
[35] Manders BG, van Herk AM, German AL. Macromol Theory Simul 1995;4:325–33.
[36] O'Driscoll KF, Kuindersma ME. Macromol Theory Simul 1994;3:469–78.
[37] Tobita H. J Polym Sci, Part B: Polym Phys 2001;39:391–403.
[38] Bouzou B, Pfluger F. Macromol Theory Simul 2003;12:243–50.
[39] He JP, Li L, Yang YL. Macromol Theory Simul 2000;9:463–8.
[40] He JP, Zhang HD, Chen JM, Yang YL. Macromolecules 1997;30:8010–8.
[41] He JP, Zhang HD, Li L, Li CM, Cao JZ, Yang YL. Polym J 1999;31:585–9.
[42] Prescott SW. Macromolecules 2003;36:9608–21.
[43] Perrier S, Barner-Kowollik C, Quinn JF, Vana P, Davis TP. Macromolecules 2002;35:8300–6.
[44] Matsumoto M, Nishimura T. ACM Trans Model Comp Simul 1998;8:3–30.
[45] Buback M, Kurz CH, Schmaltz C. Macromol Chem Phys 1998;199:1721–7.
[46] Gallot-Grubisic Z, Rempp P, Benoit H. J Polym Sci, Polym Lett Ed 1967;5:753–9.
[47] Vana P, Davis TP, Barner-Kowollik C. Aust J Chem 2002;55:315–8.
[48] McLeary JB, McKenzie JM, Tonge MP, Sanderson RD, Klumperman B. Chem Commun 2004;1950–1.
[49] Kwak Y, Goto A, Fukuda T. Macromolecules 2004;37:1219–25.
[50] Chernikova E, Morozov A, Leonova E, Garina E, Golubev V, Bui C, et al. Macromolecules 2004;37:6329–39.
[51] Feldermann A, Coote ML, Stenzel MH, Davis TP, Barner-Kowollik C. J Am Chem Soc 2004;126:15915–23.
[52] Arita T, Beuermann S, Buback M, Vana P. Macromol Mater Eng 2005;290:283–93.
[53] Dixon KW. Decomposition rates of organic free radical initiators. In: Brandrup J, Immergut EH, Grulke EA, editors. Polymer handbook. 4th ed. New York: Wiley-Interscience; 1999. p. II/1.
[54] Buback M, Huckestein B, Kuchta F-D, Russell GT, Schmid E. Macromol Chem Phys 1994;195:2117–40.
[55] Buback M, Kuelpmann A, Kurz C. Macromol Chem Phys 2002;203:1065–70.